RESEARCH ARTICLE

LncRNA ADAMTS9-AS1, as prognostic marker, promotes cell proliferation and EMT in colorectal cancer

Wanjing Chen[1] · Qian Tu[1] · Liang Yu[1] · Yanyan Xu[1] · Gang Yu[1] · Benli Jia[1] · Yunsheng Cheng[1] · Yong Wang[1]

Abstract

The long non-coding RNA antisense 1 ADAMTS9-AS1 has been reported to predict the survival in several tumors, including bladder cancer and breast cancer. However, the clinical significance and biological behaviors of ADAMTS9-AS1 in colorectal cancer (CRC) have not been reported yet. In this study, the expression of ADAMTS9-AS1 was measured in CRC tissues and cell lines using quantitative real-time PCR analysis. The clinical significance of ADAMTS9-AS1 was evaluated with Chi-squared test, Kaplan–Meier method and Cox regression analysis in CRC patients. CCK8 assay, colony formation assay, flow cytometry and transwell assay were used to explore the biological function of ADAMTS9-AS1 knockdown in CRC cell lines (SW1116 and HT29). We further explore the role of ADAMTS9-AS1 in vivo though xenograft tumor assay. Our data showed that ADAMTS9-AS1 expression level was significantly up-regulated in CRC tissues and cell lines compared with corresponding controls. High ADAMTS9-AS1 level was associated with TNM stage, lymph node invasion and worse survival prognosis. Depletion of ADAMTS9-AS1 significantly suppressed cell proliferation, G1/S transition, migration and invasion, as well as suppressed CDK4/Cyclin D1 and epithelial–mesenchymal transition (EMT). To sum up, these findings illustrated that ADAMTS9-AS1 might be a promising therapeutic target and prognostic factor for CRC.

Keywords CRC · ADAMTS9-AS1 · Prognosis · Proliferation · G1/S transition · EMT

Abbreviations

CRC	Colorectal cancer
lncRNAs	Long non-coding RNAs
EMT	Epithelial to mesenchymal transition
DMEM	Dulbecco's modified Eagle's medium
FBS	Fetal bovine serum
NC	Negative control
CCK-8	Cell Counting Kit-8
PVDF	Polyvinylidene fluoride

Wanjing Chen and Qian Tu contributed equally to this work.

✉ Yunsheng Cheng
cheng_yunailg89@yeah.net

✉ Yong Wang
Drwangyong123@126.com

1 Department of General Surgery, Economic and Technological Development District, The Second Hospital of Anhui Medical University, No.678 Furong Road, Hefei, Anhui, China

Introduction

Colorectal cancer (CRC) as a common human malignancy in digestive system ranks the leading cause of tumor-related deaths worldwide according to the latest cancer statistics data [1]. Currently, substantial progresses have been made in conventional treatments, including resection, radiation therapy, and chemotherapy, but the existence of tumor metastasis remains the leading cause of unfavorable survival prognosis [2–4]. Therefore, the identification of genes associated with CRC metastasis is of great importance to develop effective treatments and improve clinical outcomes.

Long non-coding RNAs (LncRNAs) are a novel group of RNA transcripts with more than 200 nucleotides in length, which participates in the development of cancer progression by regulating various biological process such as proliferation, cell cycle progression and migration [5, 6]. In recent years, aberrantly expressed lncRNAs are also involved in the malignant progression of CRC and their functions are successively studies. For instance, lncRNA DLEU1 contributes to CRC cell progression through regulating KPNA [7]. LncRNA ITIH4 antisense RNA 1 (ITHI4-AS1) exerts the facilitating role on CRC cell growth and metastasis both

in vitro and in vivo [8]. On the contrary, Zhang et al. demonstrated that IQCJ-SCHIP1 antisense RNA 1 (IQCJ-SCHIP1-AS1) has an indicative tumor suppressor role and appears to be a potential prognostic factor in CRC [9]. However, these regulatory mechanisms of lncRNAs in CRC are far from enough and further exploration is still needed.

With the development and application of bioinformatics analysis, a novel antisense lncRNA ADAMTS9-AS1 was initially identified to participate in the initiation and development mechanisms of epithelial ovarian cancer [10]. Li et al. [11] utilized GEO database to found ADAMTS9-AS1 stratified esophageal squamous cell carcinoma patients into high-risk and low-risk groups, which was much better than traditional clinical tumor marker. Zhu et al. [12] and Fan et al. [13] collected the patient clinical information from The Cancer Genome Atlas (TCGA) database and found ADAMTS9-AS1 was correlated with patients' survival in bladder cancer and breast cancer, respectively. Interestingly, ADAMTS9-AS1 has been reported to predict the survival for colon adenocarcinoma patients [14]. Nevertheless, to our best knowledge, the biological function of ADAMTS9-AS1 in CRC tumorigenesis has not been well studied yet.

Here, we determined the expression pattern of ADAMTS9-AS1 in CRC tissues and cell lines. Using Chisquared test, Kaplan–Meier method and Cox regression analysis, we further evaluated the clinical significance of ADAMTS9-AS1 in enrolled CRC patients. By performing loss-of-function assays, we explored the functional role of ADAMTS9-AS1 on cell proliferation, migration, invasion in vitro and tumor growth in vivo.

Materials and methods

Clinical samples

A total of paired tumor tissues and adjacent non-tumor tissues (at least 5 cm from tumor edge) were gathered from 59 cases of CRC patients who underwent surgery before radiotherapy or chemotherapy. The dissected tissues were immediately stored in liquid nitrogen and then preserved at − 80 °C until use. Basic clinical features and written informed consent were acquired from all recruited patients. The follow-up period lasted for 5 years since they received surgical resection through the telephone survey. The present study was conducted in accordance with the Declaration of Helsinki and approved by the Ethics Committee of The Second Hospital of Anhui Medical University (Approval number: AM3-289; 2015.10.15, Anhui, China).

Cell culture

Human CRC cell lines (SW1116, RKO, HT29 and HCT116) and normal human colonic epithelial cells (NCM460) were purchased from The American Type Culture Collection (ATCC, USA), which were then cultured in Dulbecco's Modified Eagle's Medium (DMEM; Gibco) containing 10% fetal bovine serum (FBS, Gibco) at 37 °C under 5% CO_2.

Cell transfection

Two different small interfering siRNAs specifically targeting ADAMTS9-AS1 (si-ADAMTS9-AS1#1: 5′-GGA ATTCAAGCTTCTACAA-3′ and si-ADAMTS9-AS1#2: 5′-CCACTGAACACATAAACAT-3′) and negative control (si-NC: 5′-UUCUCCGAACGUGUCACGUTT-3′) were synthesized by GenePharma Co, Ltd (Shanghai, China). The stable ADAMTS9-AS1 knockdown CRC cell lines were achieved through transfecting si-ADAMTS9-AS1#1 or si-ADAMTS9-AS1#2 into SW1116 or HT29 cells in six-well plates under the standard conditions for 48 h using lipofectamine 3000 (Invitrogen, Carlsbad, CA, USA) according to the manufacturer's instructions.

RNA isolation and quantitative real-time PCR

Total RNA sample was isolated from tissues or cell lines with RNAiso Reagent (Takara Bio, Shiga, Japan) and reverse transcription was performed using PrimeScrpt RT reagent Kit (TaKaRa) according to the manufacturer's instruction. Subsequently, quantitative real-time PCR was performed with specific primers for ADAMTS9-AS1 (forward: 5′-TAC TGGTTTGGACATGAGG-3′ and reverse: 5′-AAAGGG GTGTTGGCACTC-3′) and SYBR® Premix Ex Taq™ II kit (Takara) on ABI StepOnePlus system (Applied Biosystems, Foster City, CA, USA). The fold change of ADAMTS9-AS1 gene was calculated by the $2^{-\Delta\Delta Ct}$ method. Each experiment was performed in triplicate and repeated three times.

CCK-8 assay

Approximately 3000 transfected cells were plated in each well of 96-well plates and cultured at 37 °C for 24, 48, 72, 96 h. At each indicted time point, cells in each well were incubated with 10 µl of Cell Counting Kit-8 reagent (CCK-8, Dojindo, Kumamoto, Japan) for another 2 h. The absorbance was measured at 450 nm using a microplate reader (Bio-Rad, CA, USA). Each experiment was performed in triplicate and repeated three times.

Colony formation assay

Transfected cells at a density of 500 cells per well were seeded into six-well plates and cultivated for 2 weeks at 37 °C in standard culture conditions. Then the colonies (> 50 cells per colony) were fixed in 4% paraformaldehyde for 15 min, stained with 0.1% crystal violet and counted under a light microscope. Each experiment was performed in triplicate and repeated three times.

Cell cycle analysis

Transfected cells were seeded into 6-cm dishes at a density of 2×10^5 cell per well and harvested after 40 h culture. Then cells were eluted with cold PBS and fixed in 70% ice-cold ethanol at 4 °C overnight. After treatment with RNase A (100 µg/ml), cells were stained with 300 µL PBS containing 50 µg/mL propidium iodide solution for 20 min in the dark and subjected to flow cytometry analysis (BD Biosciences, San Jose, CA). Each experiment was performed in triplicate and repeated three times.

Transwell assay

For cell migration, approximately 1×10^5 transfected cells were resuspended in serum-free medium and seeded onto the upper chamber of 24-transwell plate (Corning, NY, USA). Next, complete medium with 10% FBS was added into the lower chamber. After 24 h incubation at 37 °C, migrated cells on the bottom of the lower chamber were fixed with 4% paraformaldehyde, stained with 0.1% crystal violet for 5 min and counted within three randomly selected fields via a $200 \times$ microscope (Olympus, Tokyo, Japan). The procedure of invasion assay was similar to transwell migration assay except for the transwell plate (Corning, USA) precoated with Matrigel (BD Biosciences). Each experiment was performed in triplicate and repeated three times.

Western blot analysis

Total protein sample was extracted with RIPA lysis buffer (Thermo Fisher Scientific Inc., MA, USA) and protein concentration was determined using BCA protein assay kit (Thermo Fisher Scientific Inc.,) according to the manufacturer's instruction. Equal amounts of each sample were separated by SDS-PAGE gel electrophoresis and transferred onto PVDF membranes (Millipore). Membranes blocked with TBST containing 5% skimmed milk were incubated with primary antibodies from Abcam (Cambridge, USA) of anti-CDK4, Cyclin D1, *E*-cadherin, *N*-cadherin and GAPDH at 4 °C overnight, followed by incubation with appropriate HRP-conjugated secondary antibodies at room temperature for 1.5 h. Afterwards, protein signals were visualized with an electrochemiluminescence (ECL) Kit (Sigma-Aldrich) and analyzed by ImageJ software.

Tumor xenograft model

Five-week-old male BALB/c nude mice weighing $24 \text{ g} \pm 3 \text{ g}$ were purchased from Shanghai Laboratory Animals Center of Chinese Academy of Sciences (Shanghai, China) and fed under the condition of specific pathogen-free. Then 1 ml suspension containing 2×10^7 SW1116 cells transfected with si-ADAMTS9-AS1#1 or si-NC was, respectively, subcutaneously inoculated into lower right flank of each mouse. These mice accordingly were divided into two groups (with four mice each group). Every 4 days, tumor volumes in each group were determined by digital caliper and calculated by the formula: $\text{length} \times \text{width}^2/2$. After 28 days, mice were killed and excised tumor weight was weighted. Next, the tumor tissues were collected for the analysis of ADAMTS9-AS1 expression. All the in vivo procedures were approved by the Institutional Committee for Animal Research and in accordance with the Care and Use of Laboratory Animals of The Second Hospital of Anhui Medical University (Anhui, China).

Statistical analysis

Data were expressed as mean $\pm$ SD of three biological replicates included in each experiment. Statistical analysis was performed using GraphPad Prism 6.0. Chi-squared test was used to analyze the correlations between the expression level of ADAMTS9-AS1 and patients' clinicopathological characteristics. Survival curves were plotted by Kaplan–Meier method and compared with log-rank test. Univariate and multivariate Cox regression analyses were performed to analyze the prognostic predictors affecting overall survival. Unpaired or paired Student's *t* test was used to compare between two different groups while one-way ANOVA with Dunnett post hoc test was used to evaluate the difference among multiple groups. It was considered to be of statistically significantly different, when *p* value was less than 0.05.

Results

The expression of ADAMTS9-AS1 was upregulated in CRC and associated with poor prognosis

The expression levels of ADAMTS9-AS1 were determined in 59 pairs of CRC tumor tissues and adjacent non-tumor tissues using quantitative real-time PCR analysis. The results showed that ADAMTS9-AS1 expression was significantly upregulated in CRC tissues compared with that in adjacent tissues (Fig. 1a). Similarly, ADAMTS9-AS1
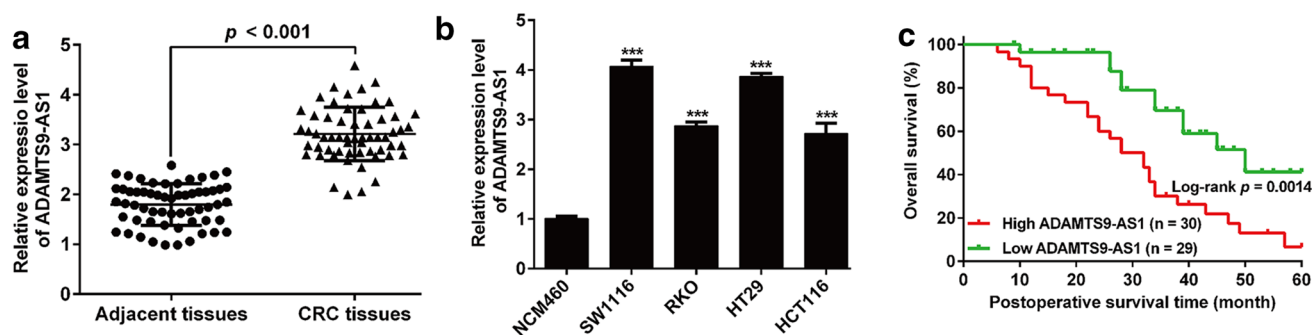
Fig. 1 The upregulation of ADAMTS9-AS1 in CRC tissues and cell lines. **a** Relative expression of ADAMTS9-AS1 in CRC tissues and adjacent normal tissues was detected by quantitative real-time PCR. **b** Relative expression of ADAMTS9-AS1 in CRC cell lines (SW1116, RKO, HT29 and HCT116) and normal human colonic epithelial cells (NCM460) was detected by quantitative real-time PCR. ***$p < 0.001$, compared with NCM460; **c** The Kaplan–Meier curves of overall survivals with high and low ADAMTS9-AS1 expressions

expressed a higher level in CRC cell lines (SW1116, RKO, HT29 and HCT116) than normal human colonic epithelial cell line NCM460 (Fig. 1b). Next, we sought to explore the clinical significance of ADAMTS9-AS1. At first, the results of Chi-squared test indicated that high expression of ADAMTS9-AS1 was correlated with TNM stage and lymph node invasion (Table 1). Next, Kaplan–Meier analysis revealed that CRC patients with high ADAMTS9-AS1 expression levels exhibited poorer overall survival (Fig. 1c). Moreover, univariate and multivariate Cox regression analysis showed that ADAMTS9-AS1 was an independent risk factor for overall survival of CRC patients (Table 2).

Depletion of ADAMTS9-AS1 suppressed CRC cell proliferation and G1/S transition

To investigate the functional role of ADAMTS9-AS1 in CRC in vitro, ADAMTS9-AS1 stably depleted SW1116 and HT29 cells were constructed by si-ADAMTS9-AS1#1 or si-ADAMTS9-AS1#2 transfection. As shown in Fig. 2a, both the siRNAs against ADAMTS9-AS1 exerted significant knockdown efficiency in SW1116 and HT29 cells. CCK-8 assay showed that depletion of ADAMTS9-AS1 by si-ADAMTS9-AS1#1 or si-ADAMTS9-AS1#2 significantly inhibited cell viability in SW1116 (Fig. 2b) and HT29 (Fig. 2c) cells. Meanwhile, we chose si-ADAMTS9-AS1#1 for the following experiments. Colony formation assay further verified the proliferation inhibitory roles of ADAMTS9-AS1 depletion by si-ADAMTS9-AS1#1 on SW1116 and HT29 cells (Fig. 2d). Furthermore, flow cytometric analysis revealed that si-ADAMTS9-AS1#1 transfection significantly elevated the percentage of cells at G0/G1 phase, accordingly reduced cell proportion at G2/M phase in SW1116 (Fig. 2e) and HT29 (Fig. 2f) cells, implying that depletion of ADAMTS9-AS1 suppressed G1/S transition in CRC cells.

Table 1 Association between ADAMTS9-AS1 expression and clinicopathological characteristics of CRC patients

Characteristics	Cases ($n = 59$)	ADAMTS9-AS1 expression level		p value
		High ($n = 30$)	Low ($n = 29$)	
Age (years)				0.506
< 60	27	15	12	
≥ 60	32	15	17	
Gender				0.243
Female	35	20	15	
Male	24	10	14	
Tumor size (cm)				0.075
< 5	41	24	17	
≥ 5	18	6	12	
TNM stage				0.044*
I-II	24	16	8	
III-IV	35	14	21	
Tumor location				0.233
Rectum	39	22	17	
Colon	20	8	12	
Tumor differentiation				0.329
Good/moderate	37	17	20	
Poor/undifferentiated	22	13	9	
Lymph node invasion				0.006*
Negative	35	23	12	
Positive	24	7	17	

CRC colorectal cancer

*$p < 0.05$

## Depletion of ADAMTS9-AS1 inhibited the migration and invasion of CRC cells

In addition to proliferation, we investigated the correlation between ADAMTS9-AS1 and CRC metastasis

Table 2 Univariate and multivariate analyses for overall survival in CRC patients

Characteristics	Univariate analysis		Multivariate analysis	
	HR (95% CI)	*p* value	HR (95% CI)	*p* value
Age (years)	1.712 (0.635–3.014)	0.312	NA	NA
Gender	0.874 (0.312–2.124)	0.745	NA	NA
Tumor size (cm)	2.314 (0.813–4.385)	0.124	NA	NA
TNM stage	2.214 (0.758–5.041)	0.185	NA	NA
Tumor location	2.584 (0.945–4.875)	0.546	NA	NA
Tumor differentiation	3.412 (1.542–6.142)	0.314	NA	NA
Lymph node invasion	3.145 (0.895–5.214)	0.003*	2.945 (0.784–4.612)	0.015*
ADAMTS9-AS1 expression	2.745 (0.784–4.978)	0.012*	2.248 (0.695–3.894)	0.032*

CRC colorectal cancer, *HR* hazard ratio, *CI* confidence interval, *NA* not analyzed

*$p < 0.05$
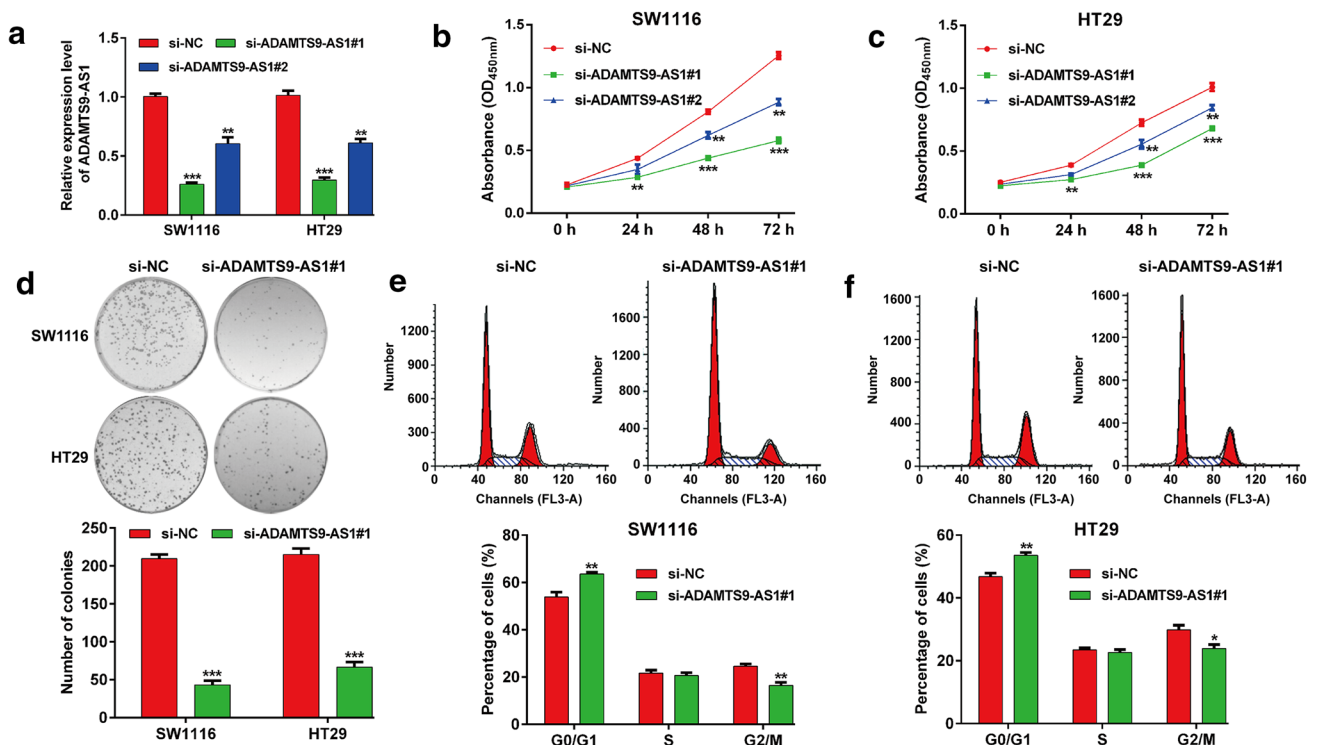
Fig. 2 Depletion of ADAMTS9-AS1 suppressed CRC cell proliferation and G1/S transition. **a** Relative expression of ADAMTS9-AS1 was determined by quantitative real-time PCR in SW1116 and HT29 cells after transfection with si-ADAMTS9-AS1#1, si-ADAMTS9-AS1#2 or si-NC. (**b, c**) CCK-8 assay was applied to analyze cell viability in transfected SW1116 and HT29 cells. (**d**) Cell proliferation was assessed by colony formation assay in SW1116 and HT29 cells after transfection with si-ADAMTS9-AS1#1 or si-NC. (**e, f**) Cell cycle distribution was analyzed by flow cytometry in SW1116 and HT29 cells after transfection with si-ADAMTS9-AS1#1 or si-NC. *$p < 0.05$, **$p < 0.01$, ***$p < 0.001$, compared with si-NC

by ascertaining the effects of ADAMTS9-AS1 on cell migration and invasion. As presented in Fig. 3a, si-ADAMTS9-AS1#1 transfection remarkably decreased the migratory cells (20.7 ± 4.5 *vs.* 104.7 ± 7.4) and invasive cells (11.0 ± 3.6 vs. 81.0 ± 3.6) compared with si-NC transfection in SW1116 cells. Similar results were also observed in HT29 cells after ADAMTS9-AS1 knockdown
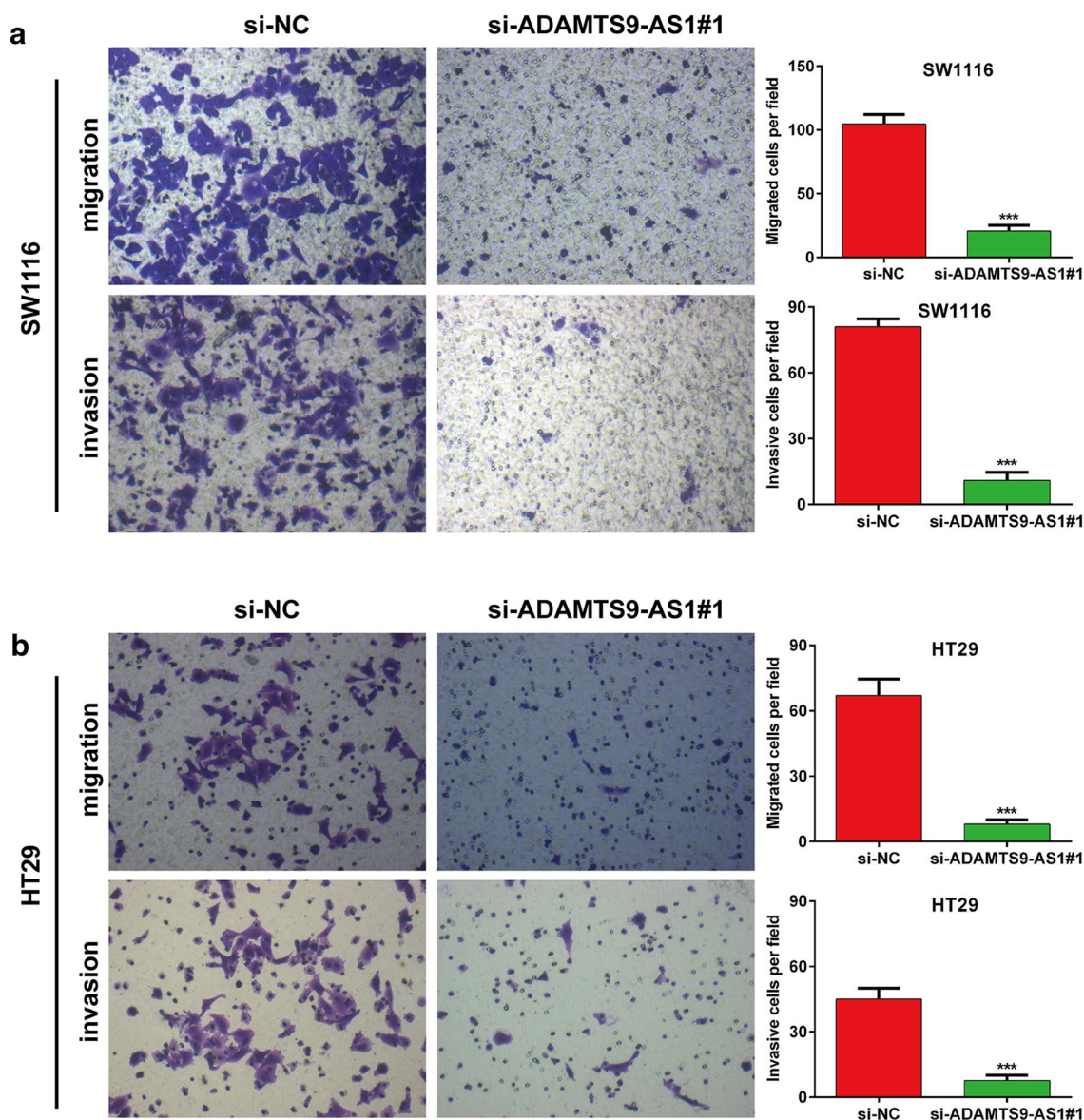
Fig. 3 Depletion of ADAMTS9-AS1 inhibited the migration and invasion of CRC cells. Transwell assay was performed to evaluate cell migration and invasion in **a** SW1116 and **b** HT29 cells after transfection with si-ADAMTS9-AS1#1 or si-NC. Representative images of migratory and invasive cells are shown in left panel and quantification of migratory and invasive cells were displayed in right panel. ***$p < 0.001$, compared with si-NC

(Fig. 3b). These results indicated that the depletion of ADAMTS9-AS1 suppressed CRC cell metastasis in vitro.

Depletion of ADAMTS9-AS1 regulated the protein expressions associated with G1/S transition and EMT

To better understand the molecular mechanisms underlying depletion of ADAMTS9-AS1 impairing cell proliferation and mobility, we explored the regulatory role of ADAMTS9-AS1 knockdown on protein expression associated with G1/S transition and EMT process by western blot analysis. As shown in Fig. 4a, ADAMTS9-AS1 knockdown downregulated the expression of CDK4 and Cyclin D1, associated with G1/S transition in SW1116 and HT29 cells. Additionally, the protein expression of *E*-cadherin was increased, while *N*-cadherin was decreased after si-ADAMTS9-AS1#1 transfection, in comparison with si-NC transfection in both SW1116 and HT29 cells (Fig. 4b).

Depletion of ADAMTS9-AS1 inhibited CRC xenograft tumor growth in vivo

Based on these in vitro findings above, a xenograft mouse model was constructed to further assess the impact of
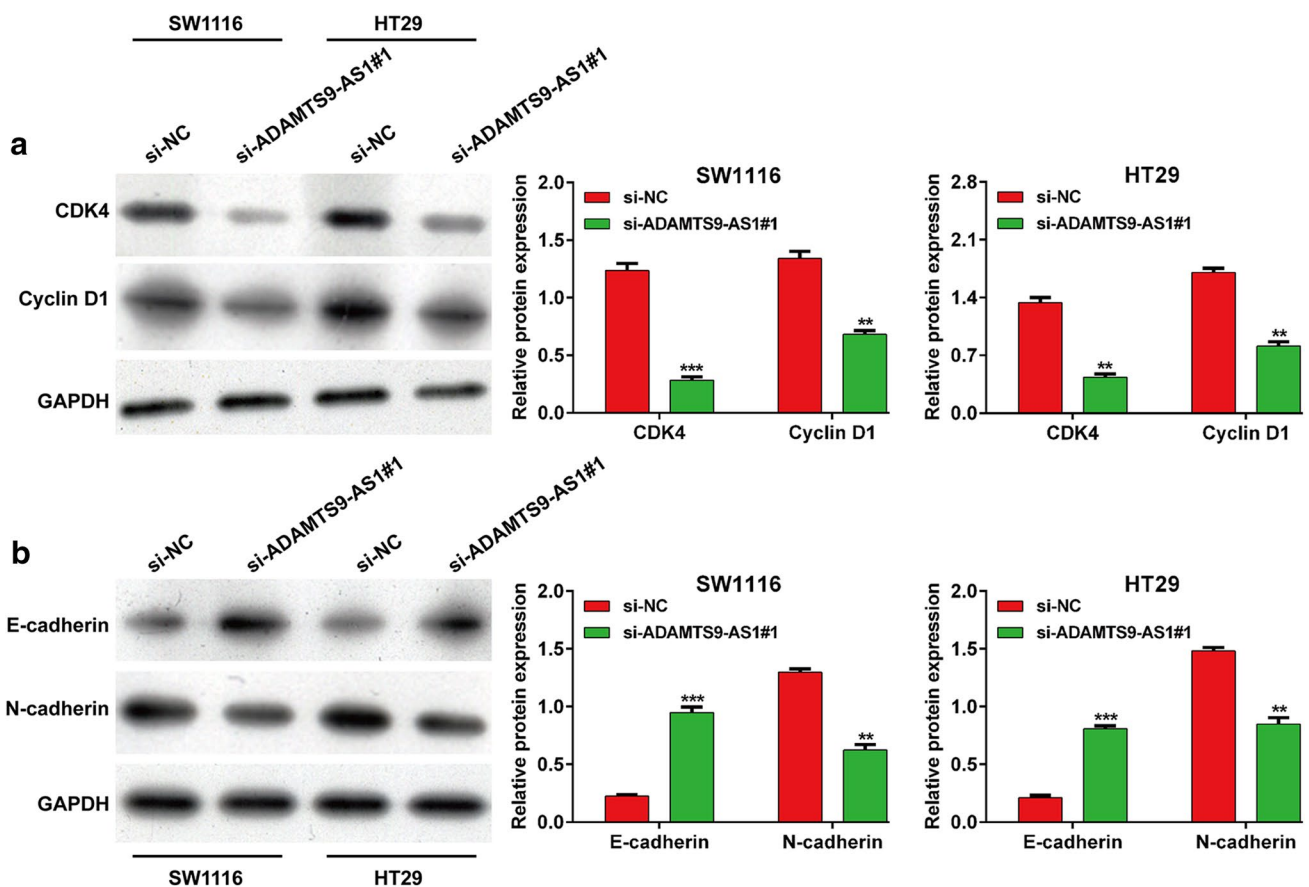
Fig. 4 Depletion of ADAMTS9-AS1 regulated the protein expressions associated with G1/S transition and EMT. **a** The protein expression of CDK4 and Cyclin D1 was measured in SW1116 and HT29 cells after transfection with si-ADAMTS9-AS1#1 or si-NC. **b** The protein expression of *E*-cadherin and *N*-cadherin was detected in SW1116 and HT29 cells after transfection with si-ADAMTS9-AS1#1 or si-NC. **p < 0.01, ***p < 0.001, compared with si-NC

ADAMTS9-AS1 on tumorigenesis in vivo. ADAMTS9-AS1 stably depleted and control SW1116 cells were injected subcutaneously into nude mice. Tumor growth rates were measured every 4 days for 28 days, and then the tumors were excised and weighed. As shown in Fig. 5a, the tumor size was smaller in si-ADAMTS9-AS1#1 group than that in si-NC group. Moreover, the time-dependent analysis showed that depletion of ADAMTS9-AS1 obviously suppressed the tumor volume compared with that in si-NC group (Fig. 5b). Then we weighed the resected tumors and found the mean tumor weight of ADAMTS9-AS1 knockdown group was significantly lower than that in the si-NC group (Fig. 5c). Quantitative real-time PCR analysis of xenograft further showed that the expression of ADAMTS9-AS1 was remarkably downregulated in si-ADAMTS9-AS1#1 group compared with si-NC group (Fig. 5d).

Discussion

In this study, we found that lncRNA ADAMTS9-AS1 was highly expressed in CRC tissues and its high expression closely correlated with TNM stage, lymph node invasion and worse survival prognosis, suggesting that ADAMTS9-AS1 was involved in CRC development. Multivariate analysis indicated that ADAMTS9-AS1 served as an independent prognostic marker for overall survival in patients with CRC. These data suggested that ADAMTS9-AS1 may serve as a potential prognostic biomarker for CRC. Consistent with our findings, lower expression of ADAMTS9-AS1 was associated with a good prognosis in bladder urothelial carcinoma patients [15]. Opposite to our data, ADAMTS9-AS1 was expressed at low levels in breast cancer [13] and prostate cancer [16] patients, which
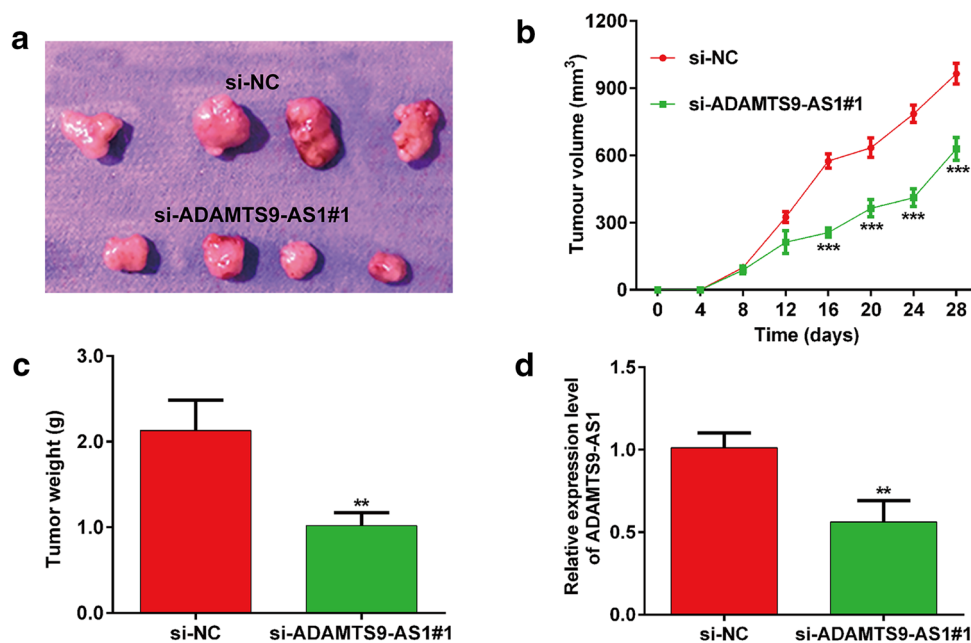
Fig. 5 Depletion of ADAMTS9-AS1 inhibited CRC xenograft tumor growth in vivo. **a** Representative images of xenograft tumors excised from nude mice derived 28 days after subcutaneous inoculation of SW1116 cells transfected with si-ADAMTS9-AS1#1 or si-NC. **b** Tumor volumes of subcutaneous tumors derived from ADAMTS9-AS1 stably depleted and control SW1116 cells were measured every 4 days. **c** Tumor weights of subcutaneous tumors derived from ADAMTS9-AS1 stably depleted and control SW1116 cells at 28 days after subcutaneous inoculation. **d** Quantitative real-time PCR detected ADAMTS9-AS1 expression level in the tumor xenografts. **p < 0.01, ***p < 0.001, compared with si-NC

serve as a novel prognostic biomarker for clinical applications. The different prognostic values of ADAMTS9-A1 in tumors might be ascribed to different tissue sources. Notably, a recent study by Xing et al. [14] who reported that ADAMTS9-AS1 expression was downregulated in colon adenocarcinoma (COAD) samples compared to those in control samples, which is controversial with our PCR data. By analyzing their data, we found some major differences might be ascribed to their relatively smaller sample size ($n = 9$), indistinct definition of paired adjacent normal tissues as well as different clinicopathological characteristics of CRC patients, when compared with our data. Anyway, this conclusion remains to be further confirmed with bigger sample size by future studies.

Our further data proved that depletion of ADAMTS9-AS1 significantly inhibited cell proliferation in vitro and tumor growth in vivo. Moreover, ADAMTS9-AS1 knockdown induced cell cycle G0/G phase arrest. It has been accepted that facilitated cell cycle progression is essential for tumor cell growth and proliferation [17]. CDK4 and Cyclin D1 play key roles cell cycle progression by mediating G1/S transition [18, 19]. CDK4 and Cyclin D1 have been widely reported to be overexpressed and correlated with tumor growth and progression [20, 21]. Consistently, we also observed the upregulated expression of CDK4 and Cyclin D1 in CRC cells. Notably, we found that depletion of ADAMTS9-AS1

resulted in the downregulated expression of CDK4 and Cyclin D1 in SW1116 and HT29 cells. Therefore, ADAMTS9-AS1 knockdown may serve as a potential therapeutic target for CRC by inhibiting cell cycle G1/S transition via downregulation of CDK4/Cyclin D1.

Furthermore, our data indicated that depletion of ADAMTS9-AS1 suppressed cell migration, invasion and epithelial–mesenchymal transition (EMT) in CRC cells. Actually, tumor metastasis accounts for approximately 90% of mortality from CRC, of which EMT is noted as a key contributing factor by increasing cancer cell mobility and invasiveness [22, 23]. EMT process is characterized by the decreased expression of epithelial markers (e.g., *E*-cadherin) and increased expression of mesenchymal markers (e.g., *N*-cadherin and vimentin) [24, 25]. Here, we demonstrated that ADAMTS9-AS1 knockdown obviously upregulated *E*-cadherin, while down-regulated *N*-cadherin expression in both SW1116 and HT29 cells. Thus, ADAMTS9-AS1 knockdown may function as tumor suppressive role in CRC metastasis by suppressive cell migration and invasion via inhibition of EMT process.

In conclusion, we manifested a novel lncRNA ADAMTS9-AS1 was upregulated in CRC and predicted poor prognosis. What's more, we demonstrated for the first time that depleted of ADAMTS9-AS1 suppressed CRC cell proliferation, G1/S transition, tumor growth, cell migration

and invasion. The present work suggests that ADAMTS9-AS1 might be a promising therapeutic target and prognostic factor for CRC.

Compliance with ethical standards

Conflict of interest The authors declare that there is no conflict of interest.

Ethics approval and consent to participate The present study was conducted in accordance with the Declaration of Helsinki and approved by the Ethics Committee of The Second Hospital of Anhui Medical University (Approval number: AM3-289; 2015.10.15, Anhui, China).

References

1. Siegel RL, Miller KD, Jemal A. Cancer statistics 2019 CA. Cancer J Clin. 2019;69:7–34.
2. Riihimaki M, Hemminki A, Sundquist J, Hemminki K. Patterns of metastasis in colon and rectal cancer. Sci Rep. 2016;6:29765.
3. Zhao L, Zhang D, Shen Q, et al. KIAA1199 promotes metastasis of colorectal cancer cells via microtubule destabilization regulated by a PP2A/stathmin pathway. Oncogene. 2019;38:935–49.
4. Chibaudel B, Tournigand C, Bonnetain F, et al. Therapeutic strategy in unresectable metastatic colorectal cancer: an updated review. Therap Adv Med Oncol. 2015;7:153–69.
5. Jiang C, Li X, Zhao H, Liu H. Long non-coding RNAs: potential new biomarkers for predicting tumor invasion and metastasis. Mol Cancer. 2016;15:62.
6. Wu C, Zhu XT, Xia L, et al. High expression of long noncoding RNA PCNA-AS1 promotes non-small-cell lung cancer cell proliferation and oncogenic activity via upregulating CCND1. J Cancer. 2020;11:1959–67.
7. Liu T, Han Z, Li H, Zhu Y, Sun Z, Zhu A. LncRNA DLEU1 contributes to colorectal cancer progression via activation of KPNA3. Mol Cancer. 2018;17:118.
8. Liang C, Zhao T, Li H, et al. Long non-coding RNA ITIH4-AS1 accelerates the proliferation and metastasis of colorectal cancer by activating JAK/STAT3 signaling. Mol Ther Nucleic Acids. 2019;18:183–93.
9. Zhang J, Bian Z, Jin G, et al. Long non-coding RNA IQCJ-SCHIP1 antisense RNA 1 is downregulated in colorectal cancer and inhibits cell proliferation. Ann Transl Med. 2019;7:198.
10. Wang H, Fu Z, Dai C, et al. LncRNAs expression profiling in normal ovary, benign ovarian cyst and malignant epithelial ovarian cancer. Sci Rep. 2016;6:38983.
11. Li Z, Yao Q, Zhao S, Wang Y, Li Y, Wang Z. Comprehensive analysis of differential co-expression patterns reveal transcriptional dysregulation mechanism and identify novel prognostic lncRNAs in esophageal squamous cell carcinoma. OncoTargets Ther. 2017;10:3095–105.
12. Zhu N, Hou J, Wu Y, et al. Integrated analysis of a competing endogenous RNA network reveals key lncRNAs as potential prognostic biomarkers for human bladder cancer. Medicine. 2018;97:e11887.
13. Fan CN, Ma L, Liu N. Systematic analysis of lncRNA-miRNA-mRNA competing endogenous RNA network identifies four-lncRNA signature as a prognostic biomarker for breast cancer. J Transl Med. 2018;16:264.
14. Xing Y, Zhao Z, Zhu Y, Zhao L, Zhu A, Piao D. Comprehensive analysis of differential expression profiles of mRNAs and lncRNAs and identification of a 14-lncRNA prognostic signature for patients with colon adenocarcinoma. Oncol Rep. 2018;39:2365–75.
15. Wang J, Zhang C, Wu Y, He W, Gou X. Identification and analysis of long non-coding RNA related miRNA sponge regulatory network in bladder urothelial carcinoma. Cancer Cell Int. 2019;19:327.
16. Wan J, Jiang S, Jiang Y, et al. Data mining and expression analysis of differential lncRNA ADAMTS9-AS1 in prostate cancer. Front Genet. 2019;10:1377.
17. Williams GH, Stoeber K. The cell cycle and cancer. J Pathol. 2012;226:352–64.
18. Goel S, DeCristo MJ, McAllister SS, Zhao JJ. CDK4/6 Inhibition in cancer: beyond cell cycle arrest. Trends Cell Biol. 2018;28:911–25.
19. Musgrove EA, Caldon CE, Barraclough J, Stone A, Sutherland RL. Cyclin D as a therapeutic target in cancer. Nat. Rev. Cancer. 2011;11:558–72.
20. Ding J, Xu K, Sun S, et al. SOCS1 blocks G1-S transition in hepatocellular carcinoma by reducing the stability of the CyclinD1/CDK4 complex in the nucleus. Aging (Albany NY). 2020;12:3962–75.
21. Tang J, Huang F, Wang H, et al. Knockdown of TPT1-AS1 inhibits cell proliferation, cell cycle G1/S transition, and epithelial-mesenchymal transition in gastric cancer. Bosn J Basic Med Sci. 2020. https://doi.org/10.17305/bjbms.2020.4470.
22. Gupta GP, Massague J. Cancer metastasis: building a framework. Cell. 2006;127:679–95.
23. Tsai JH, Yang J. Epithelial-mesenchymal plasticity in carcinoma metastasis. Genes Dev. 2013;27:2192–206.
24. Kalluri R, Weinberg RA. The basics of epithelial-mesenchymal transition. J Clin Investig. 2009;119:1420–8.
25. Miettinen PJ, Ebner R, Lopez AR, Derynck R. TGF-beta induced transdifferentiation of mammary epithelial cells to mesenchymal cells: involvement of type I receptors. J Cell Biol. 1994;127:2021–36.